Smart Structures and Systems, *Vol. 31*, *No. 2* (*2023*) *113-130*
https://doi.org/10.12989/sss.2023.31.2.113

Analytical and experimental exploration of sobol sequence based DoE for response estimation through hybrid simulation and polynomial chaos expansion

Rui Zhang [1], Chengyu Yang [2], Hetao Hou [1], Karlel Cornejo [3] and Cheng Chen*[3]

[1] *School of Civil Engineering*, *Shandong University*, *Jinan*, *Shandong*, *P.R. China*
[2] *Key Laboratory of Concrete and Prestressed Concrete Structures of the Ministry of Education*, *Tongji University*, *Shanghai*, *P.R. China*
[3] *School of Engineering*, *San Francisco State University*, *San Francisco*, *CA 94132*, *USA*

(*Received March 12*, *2022*, *Revised July 21*, *2022*, *Accepted October 15*, *2022*)

Abstract. Hybrid simulation (HS) has attracted community attention in recent years as an efficient and effective experimental technique for structural performance evaluation in size-limited laboratories. Traditional hybrid simulations usually take deterministic properties for their numerical substructures therefore could not account for inherent uncertainties within the engineering structures to provide probabilistic performance assessment. Reliable structural performance evaluation, therefore, calls for stochastic hybrid simulation (SHS) to explicitly account for substructure uncertainties. The experimental design of SHS is explored in this study to account for uncertainties within analytical substructures. Both computational simulation and laboratory experiments are conducted to evaluate the pseudo-random Sobol sequence for the experimental design of SHS. Meta-modeling through polynomial chaos expansion (PCE) is established from a computational simulation of a nonlinear single-degree-of-freedom (SDOF) structure to evaluate the influence of nonlinear behavior and ground motions uncertainties. A series of hybrid simulations are further conducted in the laboratory to validate the findings from computational analysis. It is shown that the Sobol sequence provides a good starting point for the experimental design of stochastic hybrid simulation. However, nonlinear structural behavior involving stiffness and strength degradation could significantly increase the number of hybrid simulations to acquire accurate statistical estimation for the structural response of interests. Compared with the statistical moments calculated directly from hybrid simulations in the laboratory, the meta-model through PCE gives more accurate estimation, therefore, providing a more effective way for uncertainty quantification.

Keywords: degradation; hybrid simulation; least angle regression; meta-modeling; polynomial chaos expansion; stochastic hybrid simulation; uncertainty

1. Introduction

Experimental testing is essential for engineering researchers to replicate the responses of structures and their failure during earthquakes. Findings from laboratory experiments provide the most effective means for engineers to improve their earthquake engineering practice. Traditional seismic tests include *quasi-static test*, *shaking table test*, and *pseudo-dynamic test*. Quasi-static testing (Shen *et al*. 2019), also known as cyclic testing, is most widely used in structural laboratories with a predetermined displacement history. It provides the most effective means to acquire data on structural capacity such as maximum resistance and ductility (Nakashima 2001). However, the cyclic loading protocol might not truthfully represent the seismic demand during earthquakes. Shaking table testing (Airouche *et al*. 2014, Casciati and Hamdaoui 2008) can truthfully replicate the structural system response under earthquakes but is often constrained by the table size and its payload as well as the associated experimental cost. Pseudo-dynamic testing is first introduced in the late 1960s (Hakuno *et al*. 1969). It combines digital computation with quasi-static loading thus helping overcome the size limitation of shaking table testing. The effect of loading rate on the restoring force should be of minor consequence for the pseudo-dynamic test as the structure is loaded quasi-statically (Mahin *et al*. 1989). Developed from the pseud-dynamic testing method, hybrid simulation (HS) integrates further with the substructure technique thus efficiently integrating physical experiments and computational modeling (Dermitzakis and Mahin 1985). The critical and/or complex components of a structural system that may be difficult to model numerically are built in laboratories and tested as the experimental substructures, while the rest of the structural system, generally simple to model and analyze, is numerically modeled as the analytical substructures. The coupling between substructures enables detailed examination of the entire system while imposing realistic conditions at the interfaces. The integration between numerical modeling of analytical substructures and physical testing of experimental substructures enables large- or full-scale tests in size limited structural laboratories (Nakata *et al*. 2014, Nakashima 2020). Therefore, hybrid

*Corresponding author, Ph.D., Professor,
E-mail: chcsfsu@sfsu.edu

ISSN: 1738-1584 (Print), 1738-1991 (Online)

simulation has attracted considerable interest in the past few decades (Wang *et al*. 2006, Mosqueda *et al*. 2007, Nakata *et al*. 2007, Lin *et al*. 2013, Hashemi and Mosqueda 2014, Lignos *et al*. 2014, Wang *et al*. 2020a). Moreover, HS has been extended to real-time hybrid simulation (RTHS) (Nakashima *et al*. 1992, Darby *et al*. 1999, Wu *et al*. 2006, Chen *et al*. 2009, Shao *et al*. 2011, 2014, Gao *et al*. 2013, Avci *et al*. 2020, Chen and Chen 2020, Gomez *et al*. 2020, Nakata *et al*. 2014, Wu and Wang 2014) to account for rate-dependent behavior within experimental substructures such as the MR damper (Chen *et al*. 2012, Cha *et al*. 2014, Chae *et al*. 2014, Chen *et al*. 2019) and the tuned liquid damper (Lee *et al*. 2007), and to geographically distributed hybrid simulation (Stojadinovic *et al*. 2006, Wang *et al*. 2008, Mosqueda *et al*. 2008). And Chen and Chen (2020) proposed a robust stability analysis for a general single-degree-of-freedom structure, which considers the uncertainty of servo-hydraulic system dynamics to assess the stability of a RTHS in terms of mass, damping and stiffness ratio. Researchers also proposed varied delay compensation methods (Wang *et al*. 2014, 2020b, Hayati and Song 2017). Guo *et al*. (2014) proposed an innovative way for more quantitative post-simulation evaluation of actuator tracking errors compared with existing time domain-based techniques.

Uncertainty, associated with risk, is one of major engineering points of interest and must be considered in performance assessment and practical design of civil engineering structures. Building material does not present homogeneous properties, structural elements connection varies with fatigue, and each structural component geometry is usually different from design. These uncertainties may present significant impact on seismic responses of structures. Quantification of uncertainty and evaluation of its effects on structural performance are often conducted through computational analysis of finite element modeling and methods of probability for a probabilistic measure of safety. Experimental evaluation of engineering structures through HS presents challenges to researchers on how to account for structural uncertainties, know or unknown, in laboratories. Traditional applications of HS often assume deterministic (often statistic mean) properties for the substructures. With this assumption, the structural response from HS is also deterministic for any selected ground motion. HS with deterministic parameters thus cannot help quantify the impact of structural uncertainties on seismic response and obtain its statistical characteristics for design purposes. Recent studies (Abbiati *et al*. 2015, 2018) showed that to account for inherent uncertainties within civil engineering structures, analytical substructures in HS should be characterized as stochastic instead of deterministic so that the probabilistic characteristics of structural response can be experimentally acquired through HS. This is especially true when the experimental substructures represent the critical and/or complex components of a structural system that may be difficult to model numerically. Similar challenges also exist in RTHS for which additional uncertainties due to servo-hydraulic control should be accounted for. Chen *et al*. (2017) evaluated the effect of actuator delay on the maximum displacement response from RTHS of a single degree of freedom (SDOF) structure when accounting for uncertainties in structural properties. The mean maximum displacement response is shown not necessarily equal to that when the model parameters are equal to their statistic means. More recently, Chen *et al*. (2020) compared the data-driven polynomial chaos with other generalized polynomial chaos from the aspects of the rate of error convergence when applied for uncertainty quantification of RTHS. Different statistical indicators are utilized to evaluate the accuracy of the alternative model in comparison with results from Monte Carlo simulation. Actuator delay from servo-hydraulic dynamics is demonstrated to change the sensitivity of model output from RTHS to the random variables. These research findings (Abbiati *et al*. 2015, 2018, Chen *et al*. 2017, 2020) demonstrate the need for a series of HS or RTHS to be performed in laboratories to acquire statistical structural responses to account for inherent structural uncertainties. It is imperative for HS and RTHS to be further developed for the capability of uncertainty quantification to enable probabilistic performance evaluation through laboratory experiments. This leads to *stochastic hybrid simulation* (*SHS*) and *stochastic real-time hybrid simulation* (*SRTHS*). This study will focus on stochastic hybrid simulation.

How to effectively, economically, and quantitatively account for the impact of parameter uncertainties on seismic response of structures through HS leads to the design of experimental (DoE), which aims to describe and explain the variation of information under hypothesized conditions to reflect the variation. Traditional methods for parametric uncertainty analysis are usually based on a large number of repeated experiments or simulations, such as Monte Carlo simulation (MCS) (Mooney 1997). MCS predicts the distribution of quantities of interests through repeated experiments with different parameters and its accuracy depends on the number of experiments. A sample of experimental observations is statistically similar to a sample from MCS. Therefore, the more experiments (i.e., HS in laboratories), the better experimental results account for the structural uncertainties and the more accurate experimental results capture the statistics of structural responses of interests. However, a large number of laboratory experiments will lead to formidable cost therefore is economically not feasible for DoE of SHS. Instead, the experiment design of SHS should be balanced between the number of laboratory experiments and the desired accuracy of probabilistic response prediction. In addition to MCS, several pseudo-random techniques have been developed for low-discrepancy of samples, such as Latin-Hypercube sampling (Iman *et al*. 1980), Sobol sequence (Sobol 1993), and Halton sequence (Niederreiter 1992), to effectively improve the computational efficiency. For random variables with known distributions, these low-discrepancy sequences can help achieve a faster rate of convergence close to $O(N^{-1})$, whereas the rate for MCS is $O(N^{-0.5})$. Using the Sobol sequence to sample structural uncertainties, Abbiati *et al*. (2015) computationally emulated the dynamic responses of a SDOF structure under selected ground motions and compared it with responses from traditional HS. Regular

Bouc-Wen model was applied to emulate nonlinear structural behavior under earthquakes. The Sobol sequence was shown to potentially enable SHS to obtain better accuracy through fewer experiments. In addition to these one-stage sampling approaches, adaptive sampling techniques (Jin *et al*. 2002) have also been explored in other engineering fields with an initial DoE and new experiments added in an adaptive manner.

Collapses of building structures during recent earthquakes have brought up questions as to how to determine the collapse safety margin of structures, what is the inherent collapse safety margin in code-designed structures, and how to strengthen structures to effectively augment such margin (Villaverde 2007). Although several computational analysis methods have been proposed such as equivalent SDOF systems (Takizawa and Jennings 1980, Bernal 1992), nonlinear push-over analysis (Krawinkler and Seneviratna 1998, Goel and Chopra 2004), and incremental dynamic analyses (Vamvatsikos and Cornell 2002), experimental studies have provided most truthful replication of structural collapse under earthquakes. Nakashima *et al*. (2006) tested a full-scale steel moment-resisting frame to collapse under quasi-static cyclic loading. Shake table tests have also been conducted in which structural models are tested all the way to collapse (Vian and Bruneau 2003). More recently, Ramos *et al*. (2016) applied the HS technique to evaluate system-level seismic response of a four-story steel moment frame through collapse. Compared with computational analysis and shake-table testing, HS technique provides a much more economical and realistic approach to investigate structural performance close to collapse. In earthquake engineering, collapse implies that the structural system is no longer capable to maintain its gravity load-carrying capacity in the presence of seismic effects. This makes it necessary to simulate structural response far into inelastic range in which components deteriorate in strength and stiffness (Ibarra *et al*. 2005, Lignos and Krawinkler 2011). In this study, the generalized Bouc-Wen model (Goda *et al*. 2009) is utilized to emulate strength and stiffness degradation as well as pinching of structures under earthquakes. The effect of structural nonlinearity involving degradation is first evaluated computationally on the experiment design of SHS using Sobol sequence and compared with traditional HS using MCS. Hybrid simulations of a SDOF structure with mass and damping uncertainties are further conducted in the laboratory to validate the findings from computational analysis.

2. Meta-modeling and polynomial chaos expansion

To acquire better statistical estimates of structural response quantities from a limited number of hybrid simulation, metal-modeling technique is used in this study. Meta-model, also known as surrogate model, can be obtained by fitting the responses from a small number of samples (Blanning 1975). A meta-model can thus be considered as a simplified model of an actual model of structural components or systems. A wide scope of meta-models is available in the existing literatures such as Kriging (Martin and Simpson 2005, Gaspar *et al*. 2014), support vector machines (Bourinet 2016), artificial neural networks (Chojaczyk *et al*. 2015, Hurtado and Alvarez 2001), radial basis functions (RBFs) (Fang and Horstemeyer 2006), polynomial chaos expansion (PCE) (Blatman and Sudret 2010), high-dimensional model representation (Chowdhury and Rao 2009). Among various meta-modeling approaches, surrogate modeling based on PCE has attracted considerable interest due to its interpretation and versatility advantages. Based on the homogenous chaos theory (Wiener 1938), PCE has demonstrated higher efficacy compared with MCS method when uncertainty quantification is conducted with limited samples (Isukapalli *et al*. 1998). Original PCE method uses Hermite polynomial as it has an exponential type of optimal convergence rate towards random variables with Gaussian distribution. Xiu and Karniadakis (2002) later proposed a generalized PCE method to extend Wiener's approach to continuous and discrete polynomials.

Assume a finite number of input random variables as $\mathbf{X} = \{X_1, \ldots, X_M\}$, and a response Y with finite variance as

$$Y = F(X) \tag{1a}$$

Suppose that every random variable X_i (i = 1…M) is defined by its probability density function $f_{X_i}(x_i)$, the polynomial chaos expansion of Y can be expressed as

$$Y = \sum_{j \in N} y_j \Psi_j(\boldsymbol{X}) \tag{1b}$$

where $\Psi_j(X)$ (j = 1…N) are orthonormal multivariate polynomials; and y_j are scalar coefficients. In practice, Eq. (1b) is often truncated to a finite series for the benefits of applications. A common method is to have all M-dimensional multivariate polynomials of total degree $|\alpha| \leq p$, where p is the maximum degree defined; $A^{M,p} = \{\alpha: |\alpha| < p\}$ is the truncated set of multi-indices.

$$Y = \sum_{\alpha \in A^{M,p}} y_\alpha \Psi_\alpha(X) + \varepsilon \tag{1c}$$

where ε is the truncation error and defined as

$$\mathrm{E}[\varepsilon^2] \stackrel{\text{def}}{=} E\left[\left(Y - \sum_{\alpha \in A^{M,p}} y_\alpha \Psi_\alpha(X)\right)^2\right] \tag{2}$$

where E represents expectation. Eq. (1c) is called full PCE model when the maximum value of α is equal to the total degree of multivariate polynomials. However, the number of basis polynomials increases with the number of input variables due to the *curse-of-dimensionality*. This study uses the least angle regression (LARS) (Blatman and Sudret 2011) to include only the most influential polynomials in the so-called sparse PCE model. Specifically, the calculation of coefficient y_α can be considered as a minimization problem

$$y_\alpha = argmin\ \mathbf{E}\left[\left(F(X) - \sum_{\alpha \in A^{M,p}} y_\alpha \Psi_\alpha(X)\right)^2\right] \quad (3)$$

If the expected part of above formula is replaced by the estimated value in Eq. (1c), the approximate value of the coefficients can be obtained from the training set

$$\widehat{y_a} = argmin \frac{1}{N}\sum_{i=1}^{N}\left(MF\left(x^{(i)}\right) - y_a^T \Psi_a\left(x^{(i)}\right)\right)^2 \quad (4)$$

where $\mathrm{X} = \{\mathrm{x}^{(1)}, \ldots, x^{(N)}\}$ is a set of samples (also referred to as training set in this study) from input uncertain parameters; $\mathrm{y} = \{y^{(1)} = \mathrm{F}\left(x^{(i)}\right), \ldots, y^{(N)} = \mathrm{F}(x^{(N)})\}$ is the response vector of corresponding training set; N is the number of elements in the training set; and $\Psi_\alpha\left(x^{(i)}\right) = \{\Psi_{\alpha 1}\left(x^{(1)}\right), \ldots, \Psi_{\alpha p}\left(x^{(p)}\right)\}$ contains the corresponding multivariate polynomials of all samples except the i^{th} sample. The calculation of PCE coefficient y_α is carried out in this study using the Matlab based toolbox UQ-Lab (Marelli and Sudret 2015). The *cross-validation* technique, also known as out-of-sample testing, is used in this study to estimate the error of the PCE model calculated based on the training set. More specifically, the leave-one-out (LOO) error is used in this study. For the meta-model $F^{PC\backslash i}(X)$ established by other elements except the i^{th} element $x^{(i)}$ in the training set, the predicted residual Δ_i for the i^{th} point $x^{(i)}$ can be calculated as

$$\Delta_i = F\left(x^{(i)}\right) - F^{PC\backslash i}\left(x^{(i)}\right) \quad (5)$$

The LOO error is then defined as

$$\varepsilon_{LOO} = \frac{1}{N}\sum_{i=1}^{N}\Delta_i^2 \quad (6a)$$

To enable the comparison for models with different scales, the LOO error is normalized by the response variance to assess the fitting of PCE meta-model to the training set, which can be expressed as

$$\epsilon_{LOO}^* = \frac{\epsilon_{LOO}}{Var(Y)} \quad (6b)$$

Alternatively, Eq. (6b) can be computed fast in single training process as

$$\varepsilon_{LOO} = \frac{1}{N}\sum_{n=1}^{N}\left(\frac{F\left(x^{(n)}\right) - F^{PC}\left(x^{(n)}\right)}{1 - h_n}\right)^2 \quad (6c)$$

where $\mathrm{h_n}$ is the n^{th} diagonal element of the matrix. More details of computation for the PCE coefficients can be referred to Blatman and Sudret (2011). After the PCE model is established, the mean and the variance of the structural response output can be calculated as

$$\mathrm{E}[F^{PC}(X)] = E\left[\sum\nolimits_{\alpha \in A} y_a^T \Psi_a(X)\right] = \hat{y}_0 \quad (7a)$$

$$\mathrm{E}[(F^{PC}(X) - \hat{y}_0)^2] = \sum_{\substack{\alpha \in \mathcal{A} \\ \alpha \neq 0}} \hat{y}_\alpha^2 \quad (7b)$$

3. Hybrid simulation of a SDOF structure with nonlinear behavior involving degradation

A single degree of freedom (SDOF) structure is considered in this study, of which the equation of motion is defined as

$$m\ddot{x}(t) + c\dot{x}(t) + r(t) = -m\ddot{x}_g(t) \quad (8a)$$

where $\dot{x}(t)$ and $\ddot{x}(t)$ are the velocity and acceleration response, respectively; $\ddot{x}_g(t)$ is the ground motion; m and c are the mass and inherent viscous damping of the SDOF structure, respectively; and r(t) is the nonlinear restoring force of the SDOF structure. Eq. (8a) can be reformulated as

$$\ddot{x}(t) + 2\xi\omega_n\dot{x}(t) + \frac{r(t)}{m} = -\ddot{x}_g(t) \quad (8b)$$

where ω_n and ξ are the natural frequency and the viscous damping ratio of the SDOF structure, respectively. To enable hybrid simulation, the part of structure associated with restoring force $r(t)$ is taken as experimental substructure and the rest of the structure is taken as analytical substructure. It is also assumed in this study that the restoring force in Eqs. (8a) and (8b) is not rate-dependent so that the experiments do not need to be executed in a real-time manner.

3.1 Generalized Bouc-Wen Model

Different hysteretic models have been proposed to emulate nonlinear behavior with degradation, such as the smooth hysteretic degrading model (Sivaselvan and Reinhorn 2000), the degradation model based on dissipated hysteretic energy (Song and Pincheira 2000) and more recently the Modified Ibarra-Medina-Krawinkler Deterioration Model (Ibarra *et al*. 2005, Lignos and Krawinkler 2011). In this study, the generalized Bouc-Wen model (Goda *et al*. 2009) is utilized to emulate the strength and stiffness degradation behavior for the experimental substructure. The equation of motion in Eq. (8b) can be revised as

$$\ddot{\mu} + 2\xi\omega_n\dot{\mu} + \alpha{\omega_n}^2\mu + (1-\alpha){\omega_n}^2\mu_z = -\frac{\ddot{x}_g}{\varphi u_0} \quad (8c)$$

where α is the ratio of post-yield stiffness to initial stiffness; the normalized yield strength φ and ductility μ are defined as $\varphi = x_y/x_0 = f_y/f_0$; $\mu = x/x_y$ and $\mu_z = z/u_y$, respectively; x_0 and f_0 are the maximum displacement and hysteretic force under the selected ground motion; and x_y and f_y are the yield displacement and yield force, respectively. The constitutive equation of the generalized Bouc-Wen model is defined as

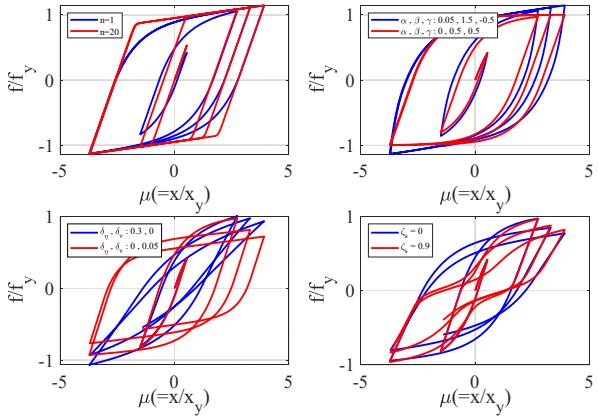

Fig. 1 Hysteretic behavior with different parameter values of generalized Bouc-Wen model

Table 1 Definition of uncertainty for HS parameters

	X_{min}	X_{max}	Mean	Standard deviation	C. O. V
ω_n (rad/sec)	5.44	7.02	6.28	0.44	0.07
ζ	0.01	0.03	0.02	0.0029	0.145

$$\dot{\mu}_z = \frac{h(\mu_z,\varepsilon_n)}{1+\delta_n\varepsilon_n}[\dot{\mu} - (1+\delta_v\varepsilon_n)(\beta|\dot{u}||\mu_z|^{n-1}\mu_z + \gamma|\dot{u}||\mu_z|^n)] \tag{9a}$$

$$h(\mu_z,\varepsilon_n) = 1-\zeta_s(1-e^{-p\varepsilon_n})\,exp\left(-\left(\frac{\mu_z\,sgn(\dot{\mu}) - q/\{(1+\delta_v\varepsilon_n)(\beta+\gamma)\}^{\frac{1}{n}}}{\left(\lambda+\zeta_s(1-e^{-p\varepsilon_n})\right)\left(\psi+\delta_\psi\varepsilon_n\right)}\right)^2\right) \tag{9b}$$

$$\varepsilon_n = (1-\alpha)\int_0^T \dot{\mu}\mu_z\,dt \tag{9c}$$

where t is the time; β, γ and n are parameters that control the shape of the hysteretic curve; δ_v and δ_n are parameters that control the stiffness and strength degradation, respectively; $h(\mu_z,\varepsilon_n)$, ζ_s, p, q, ψ and δ_ψ are parameters that control the pinching effect; and ε_n is the energy consumed by hysteresis. Fig. 1 shows the effect of model parameter values on the hysteretic behavior of the generalized Bouc-Wen model. It can be observed that degradation in stiffness and strength as well as pinching can be well emulated with properly selected parameter values. It can also be observed that ductility plays an important role for the degradation behavior, which however is beyond the scope of this study.

3.2 Model parameter uncertainty

The number of parameters in Eq. (8c) adds up to fifteen and uncertainties could exist in all these parameters. Mass, stiffness and damping are the three key parameters that can reflect the dynamic characteristics of the structure. It can be seen that mass is not a variable in Eq. (8c). For the purpose of analysis and also to avoid the curse-of-dimensionality, the structural uncertainties in this study are assumed from the linear elastic stiffness k (which translates to the natural frequency ω_n in Eq. (8c)) and the inherent damping ratio ζ. The nominal natural frequency and the nominal inherent viscous damping ratio are assumed to be 1.0 Hz and 2% for the SDOF structure. Table 1 provides assumed uncertainties of parameters ω_n and ζ, where both are assumed to follow normal distribution with bounded values. It is worth noting that the uncertainties in Table 1 are assumed for the purpose of analysis in this study and different uncertainties can be assigned for the parameters when historical data and statistics are available.

Samples of the random variables associated with structural uncertainties are required to account for uncertainties in DoE for stochastic hybrid simulation. As discussed in the introduction, different sampling techniques have been proposed for structural reliability assessment in

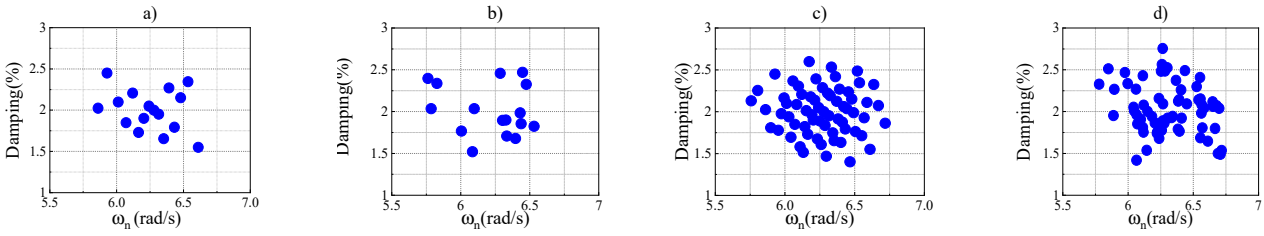

Fig. 2 Comparison of samples: (a) and (c) 16 and 64 from Sobol Sequence; (b) and (d) 16 and 64 from Monte Carlo sampling

Table 2 Statistics of samples from sobol sequence

Sample number	X_{min}		X_{max}		Mean		Standard deviation		C. O. V.	
	ω_n	ζ	ω_n	ζ	ω_n	ζ	ω_n	ζ	ω_n	ζ
16	5.86	0.016	6.61	0.025	6.25	0.02	0.047	0.0029	0.008	0.145
32	5.81	0.015	6.67	0.025	6.26	0.02	0.048	0.0029	0.008	0.145
64	5.76	0.014	6.72	0.026	6.27	0.02	0.048	0.0029	0.008	0.145
128	5.72	0.013	6.76	0.027	6.27	0.02	0.049	0.0029	0.008	0.145

the past. In this study, the pseudo-random Sobol sequence is used due to its low discrepancy. Fig. 2 shows the comparison of samples of ω_n and ζ between Monte Carlo Sampling and Sobol sequence for the numbers of samples equal to 16 and 64.

As can be observed, the samples from Sobol sequence scatter more uniformly over the defined sample space. Table 2 presents the statistics for different number of Sobol sequence samples.

It can further be observed that statistics of the Sobol sequence samples match the defined uncertainties in Table 1 with the increase of the number of samples.

3.3 Computational simulation matrix

Previous studies have shown that ground motion uncertainties could be dominant for structural response prediction under earthquakes. This study therefore selects two ground motions to explore the effect of record-to-record variation on the DoE of SHS. Fully characterizing the effect of record-to-record variation is however beyond the scope of this study. The time histories of two ground motions, referred to as GM1 and GM2, are presented in Fig. 3, where GM1 is recorded at El Centro station during the 1940 El Centro earthquake and GM2 is recorded at the Shin-Osaka station during the 1995 Kobe earthquake.

To evaluate the influence of degradation close to structural collapse, and in order to study the deformation degree of structure more intuitively (the maximum displacement of the structure does not increase monotonously with the increase of PGA), the two selected ground motions are scaled for the ductility of the SDOF structure to vary between 1 and 10 for the SDOF structure with nominal values of natural frequency and viscous damping ratio. And the scales of Ground motion GM01 and GM02 are shown in Tables 3 and 4. In order to make the

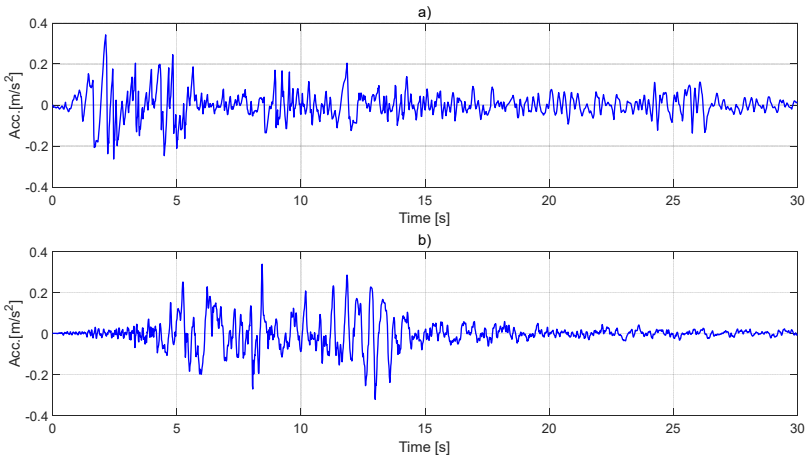

Fig. 3 Time history of selected ground motions: (a) GM1; (b) GM2

Table 3 Scales of ground motion GM01

Ductility	1	2	3	4	5	6	7	8	9	10
Case 1: no degradation	0.18	0.35	0.55	0.82	1.07	1.21	1.36	1.47	1.53	1.65
Case 2: strength degradation only	0.18	0.35	0.55	0.65	0.74	0.88	1.03	1.34	1.44	1.52
Case 3: stiffness degradation only	0.18	0.35	0.45	0.55	0.65	0.80	1.10	1.25	1.40	1.50
Case 4: both degradation	0.18	0.35	0.49	0.60	0.71	0.81	0.89	1.06	1.18	1.23
Case 5: Pinching and both degradation	0.18	0.33	0.53	0.72	0.92	1.10	1.38	1.46	1.56	1.65
Case 6: Pinching only	0.18	0.30	0.53	0.69	0.87	1.02	1.12	1.24	1.47	1.57

Table 4 Scales of ground motion GM02

Ductility	1	2	3	4	5	6	7	8	9	10
Case 1: no degradation	1.20	2.40	3.75	4.70	6.10	7.25	8.30	9.50	10.7	11.9
Case 2: strength degradation only	1.20	2.40	3.75	4.70	6.10	7.00	8.20	9.20	10.2	11.3
Case 3: stiffness degradation only	1.20	2.28	3.25	4.30	5.50	6.60	7.85	9.50	10.4	11.69
Case 4: both degradation	1.20	2.28	3.40	4.60	5.80	6.99	8.30	9.30	10.7	11.75
Case 5: Pinching and both degradation	1.20	2.05	3.80	5.30	6.20	7.30	8.40	9.50	10.5	11.80
Case 6: Pinching only	1.20	2.05	3.40	4.90	5.90	6.90	8.00	8.90	10.2	11.50

Table 5 Bouc-Wen Parameters for computational simulations

Ductility	α	β	γ	n	δ_v	δ_η	ς_s
Case 1: no degradation	0.05	0.5	0.5	1	0	0	0
Case 2: strength degradation only	0.05	0.5	0.5	1	0.05	0	0
Case 3: stiffness degradation only	0.05	0.5	0.5	1	0	0.3	0
Case 4: both degradation	0.05	0.5	0.5	1	0.05	0.1	0
Case 5: Pinching and both degradation	0.05	0.5	0.5	1	0.05	0.1	0.9
Case 6: Pinching only	0.05	0.5	0.5	1	0	0	0.9

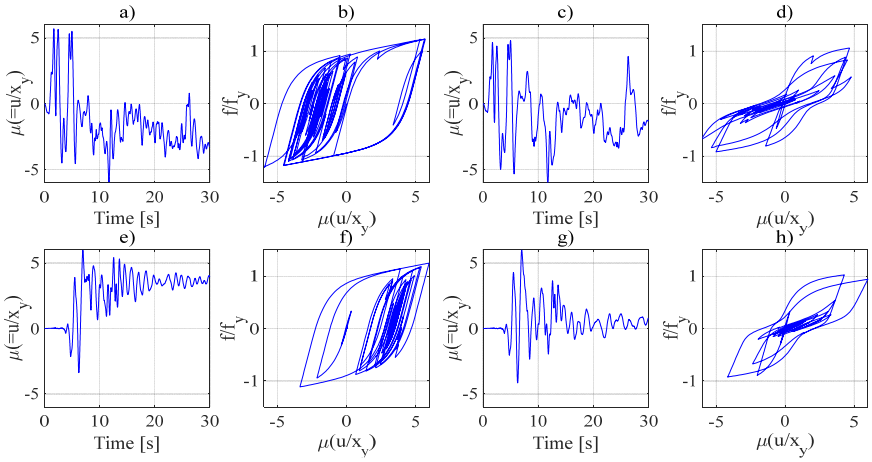

Fig. 4 Time history responses of SDOF structure (ω_n = 6.28 and ζ = 0.02): (a) and (b): case 1 under GM1; (c) and (d): case 5 under GM1; (e) and (f): case 1 under GM2; (g) and (h): case 5 under GM2

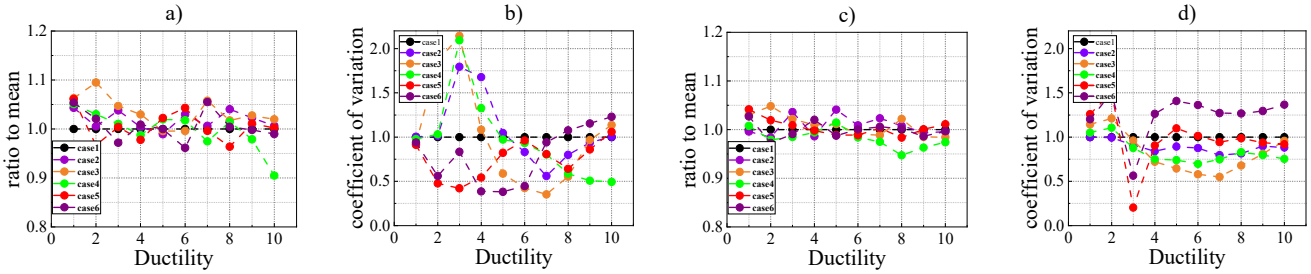

Fig. 5 Statistic mean and variance of μ from MCS: (a) and (b): GM1; (c) and (d): GM2

ductility of structures are on the same level under GM01 and GM02, we scaled ground motions. The different scales between GM01 and Gm02 can be attributed to the different PGA values and different SDOF structural responses.

Six cases are considered in this study including no degradation, strength degradation only, stiffness degradation only, both degradations, pinching only, and both degradation plus pinching, which will be referred to as case 1 through case 6, respectively. Table 5 presents the parameter values of all six cases for the computational simulations.

Fig. 4 presents typical responses of the SDOF structure for the cases of 1 and 5 when the two random parameters take mean values and the two ground motions are scaled to achieve displacement ductility demand around 6. Hysteretic behavior without degradation can be observed in Figs. 4(b) and 4(f) while degradation and pinching occur in Figs. 4(d) and 4(h). Different structural responses can also be observed in Figs. 4(a) and 4(c), Figs. 4(e) and 4(g) due to different nonlinear behavior.

Research shows that maximum story drift is a dominant factor that contributes to structural damage during earthquakes. This study therefore considers the maximum displacement ductility demand as the main structural response quantity of interest from hybrid simulation in the laboratories. For the purpose of evaluation, Monte Carlo simulation of 10^5 times is conducted first to provide benchmark statistical moments of maximum displacement ductility. Values of mean and coefficient of variance from MCS are normalized by those of case 1 and presented in Fig. 5 for GM1 and GM2. Although the two ground motions are both scaled for case 1 with mean values of ω_n and ζ, differences can be observed in the mean maximum displacement ductility in MCS results. This can be

attributed to the fact that nonlinear structural response varies due to structural uncertainties. Different structural nonlinearity is also observed in Fig. 5 to affect the COV of maximum displacement ductility. It can also be observed that the mean and COV for GM2 are consistently smaller than those for GM1, implying that the effect of structural uncertainties varies for different ground motion inputs. These warrant the research needs for stochastic hybrid simulation.

3.4 PCE meta-models for maximum displacement ductility

Following a limited number of simulations or experiments, there are two main ways to estimate the statistics of structural responses quantities of interests. One is to calculate the mean and variance directly from results from simulations or experiments. The other is to establish a meta-model using the acquired information. PCE meta-models are established in this study for the maximum displacement ductility using different sets of samples from Sobol sequence. The Matlab based toolbox UQ-Lab (Marelli and Sudret 2015) is used to compute the PCE coefficients and determine the optimal degree of PCE model based on the LOO errors. This study considers different numbers of Sobol sequence samples including 16, 32, 64, 128 and 256. It is worth noting that a total of 128 or 256 or even 64 experiments would be too much for researchers aiming to acquire statistics of structural response quantities through stochastic hybrid simulations in laboratories. For the purpose of analysis, here we want to explore the convergence of structural response statistics with the increase of the number of experiments. Fig. 6 presents the LOO errors of the PCE models for the ground motion GM1 with the increase of nominal displacement ductility demand. Generally, the increase in the number of Sobol sequence samples leads to smaller LOO errors for minor ductility ($\mu \leq 4$) as shown in Figs. 6(a)~(d). Take μ around 3 in Fig. 6(c) for example, the LOO error decreases from 0.06 to 0.04 when the sample number increases from 16 to 32, and then converges to 0.026 when the sample number continues to increase to 256. This can be attributed to the fact that adding more experiments, if designed properly, enables more accurate PCE meta-models to precisely capture the statistic characteristics of structural responses under uncertainties. However, when the SDOF structure involves both strength and stiffness degradation and/or pinching, the LOO error in Figs. 6(e)~6(f) seems not correlated with the number of Sobol sequence samples. For μ around 3, the minimum LOO error occurs for sample number equal to 16 in Fig. 6(e) and for sample number equal to 64 in Fig. 6(f). For μ around 3 in Fig. 6(e), increasing the sample points from 16 to 32 and from 64 to 128 leads to the increased LOO error from 0.16 to 0.3, 0.09 to 0.85 respectively. Increasing the number of Sobol sequence samples is observed to not necessarily lead to smaller LOO error. This implies that the predefined one-stage sampling might not be efficient for the complex nonlinear behavior. For moderate ($4 \leq \mu \leq 8$) and significant ductility ($8 \leq \mu \leq 10$), it becomes more obvious that LOO errors do not necessarily increase or decrease monotonically with either the ductility demand or the number of samples. For example, the minimum LOO error for case 1 occurs for the sample number equal to 256 for μ around 6 but for the sample number equal to 32 for μ around 10. For the same case, the LOO errors are about the same for all different number of samples for the ductility around 4 and 9. Similar observations can also be made for other cases in Fig. 6. This again implies that for moderate and significant ductility the increase of Sobol sequence samples does not necessarily reduce the LOO errors of the PCE models, or the increase of the number of hybrid simulations will not lead to more accurate PCE models. When the structure develops moderate or significant nonlinear behavior, some of the

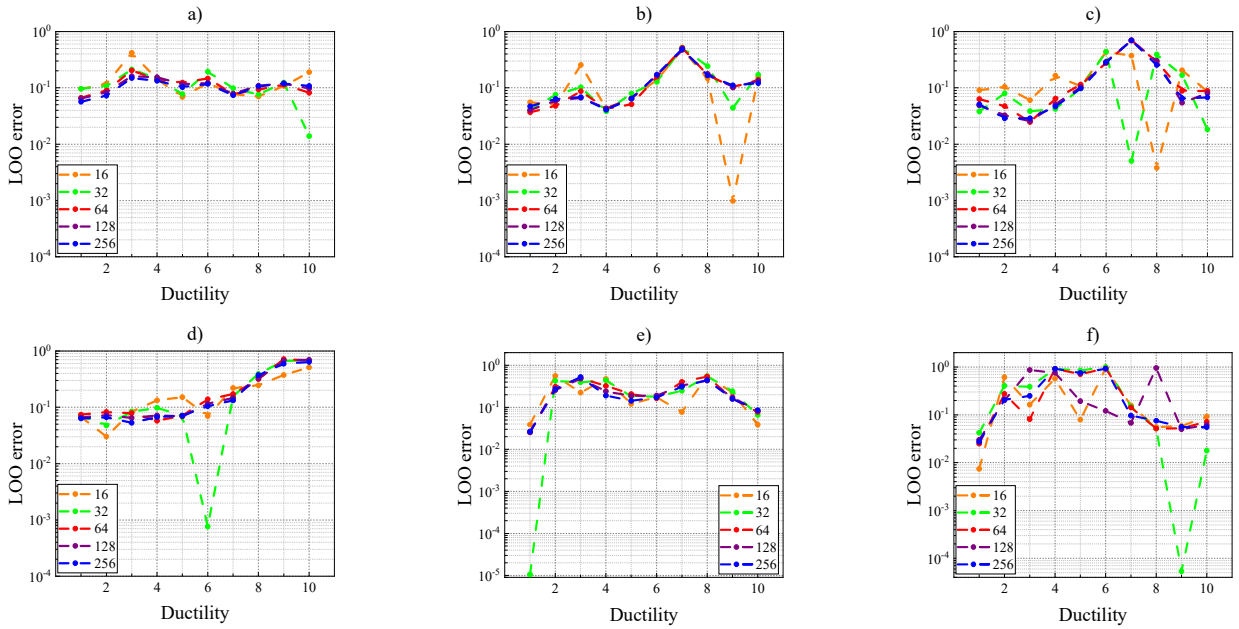

Fig. 6 LOO errors vs. Ductility for GM1: (a) case 1; (b) case 2; (c) case 3; (d) case 4; (e) case 5; (f) case 6

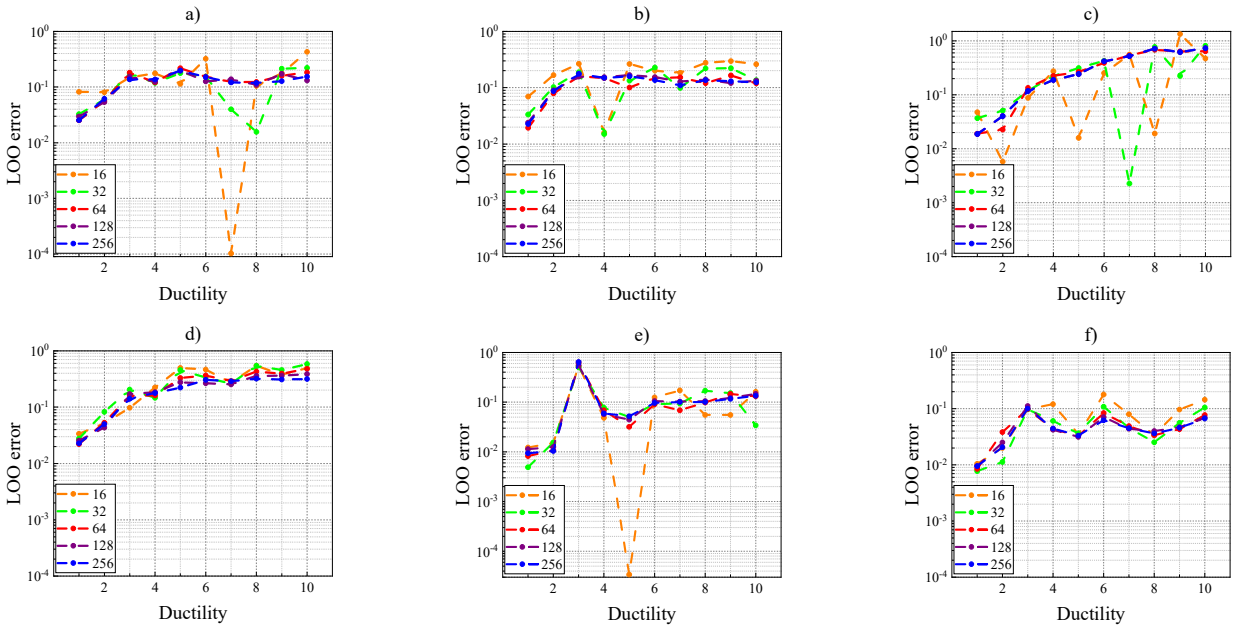

Fig. 7 LOO errors vs. Ductility for GM2: (a) case 1; (b) case 2; (c) case 3; (d) case 4; (e) case 5; (f) case 6

Table 6 Summary of LOO error for PCE meta-models

GM	Sample	Case 1	Case 2	Case 3	Case 4	Case 5	Case 6
GM1	$(LOO)_{min}$	0.0139	9.84e-4	0.0038	7.64e-4	1.05e-5	0.2419
	Sample for $(LOO)_{min}$	32	16	16	32	32	32
	$(LOO)_{max}$	0.4175	0.099	0.7009	0.7156	0.5582	1.0009
	Sample for $(LOO)_{max}$	16	32	64	64	16	32
GM2	$(LOO)_{min}$	1.03e-4	0.015	0.0023	0.0221	3.39e-5	0.0077
	Sample for $(LOO)_{min}$	16	32	32	64	16	32
	$(LOO)_{max}$	0.4277	0.2969	1.3355	0.5818	0.6436	0.1244
	Sample for $(LOO)_{max}$	16	16	16	32	256	16

LOO errors are observed to increase up to 1.0. Table 6 presents maximum and minimum LOO errors of the PCE meta-models for all six cases. Again, it can be observed that the maximum or the minimum LOO does not necessary occurs for the minimum or maximum number of samples. Comparing all the six cases in Fig. 6, the LOO errors for case 1 in Fig. 6(a) are observed to have the least variation, while the case 5 in Fig. 6(e) which involves both stiffness and strength degradation as well as pinching has the largest variation in LOO errors. This implies that the degradation and pinching have impact on accuracy of the PCE meta-models thus the number of hybrid simulations to acquire accurate estimates of structural response statistics.

Fig. 7 presents the LOO errors of the PCE meta-models for the ground motion GM2. Different from those presented in Fig. 6 for GM1, the LOO errors of case 2 in Fig. 7(b) shows the least variation, while the case 6 in Fig. 6(f) which considers pinching only has the largest variation. This can be attributed to the record-to-record variation and also indicate that uncertainty from ground motions plays an important role in DoE for SHS. Similar to the observations made from Fig. 6, the LOO errors decrease with the increase of the number of sample points for minor ductility ($\mu \leq 4$) of cases in Figs. 7(a)~(d), and then maintain almost same for moderate ductility. For significant ductility, the number of sample points is shown not directly related to LOO errors when the number of samples is greater than 32. For cases in Figs. 7(d)~(f), the reduction of LOO errors is observed not correlated with the increase of sample points. The LOO errors for case 4 in Fig. 6(d) is observed to increase monotonically with respect to the ductility, while the LOO errors for case 5 in Fig. 6(e) are observed to have significant fluctuation. The observations from Figs. 6 and 7 show that the accuracy of PCE meta-models is indeed affected by different nonlinear behavior. This brings the challenge for how to efficiently conduct DoE for stochastic hybrid simulation. Table 6 summarizes the maximum and minimum LOO error for all six cases and the corresponding number of Sobol sequence samples. Interestingly, all maximum and minimum LOO errors occur for the number of samples no more than 64. It is again observed that the LOO errors vary for the two ground motions due to the record-to-record variation.

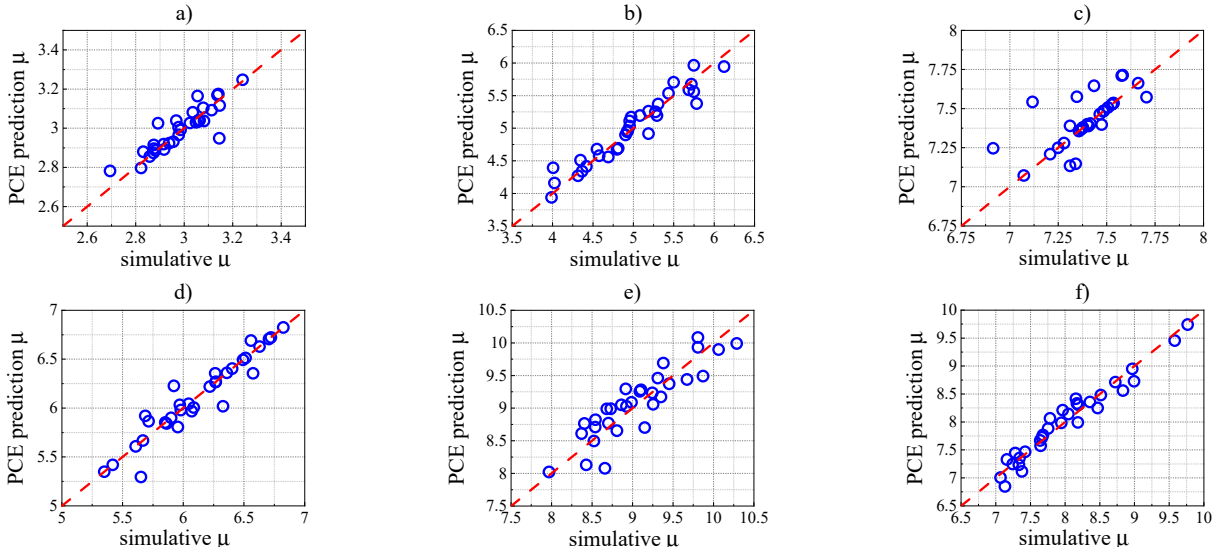

Fig. 8 Prediction of μ from PCE meta-models from 32 samples: (a) case 1, μ = 3; (b) case 2, μ = 5; (c) case 3, μ = 7; (d) case 4, μ = 6; (e) case 5, μ = 9; (f) case 6, μ = 8

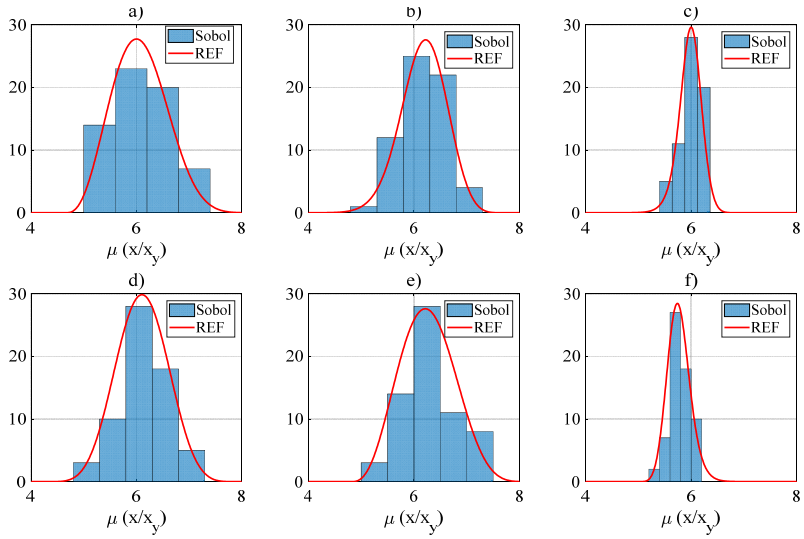

Fig. 9 Histograms of μ for GM1 with 64 samples: (a) case 1; (b) case 2; (c) case 3; (d) case 4; (e) case 5; (f) case 6

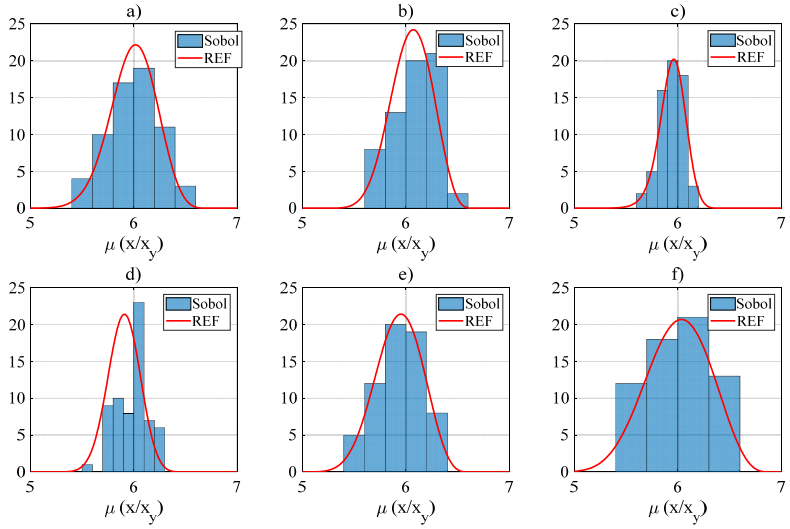

Fig. 10 Histograms of μ for GM2 with 64 samples: (a) case 1; (b) case 2; (c) case 3; (d) case 4; (e) case 5; (f) case 6

Fig. 8 presents the validation for the accuracy of selected PCE meta-models for the computational analysis with GM1 and 32 Sobol sequence samples. These PCE meta-models are shown in Fig. 6 to have corresponding LOO errors of 0.2, 0.08, 0.005, 0.0007, 0.25 and 0.005, respectively. The PCE predictions are observed to generally agree well with corresponding values from computational simulation. For the two cases with relatively large values of LOO in Figs. 8(a) and 8(e) good agreement can still be observed. This implies that the PCE meta-models in Figs. 6 and 7 provide good accuracy in the prediction of maximum displacement ductility. Figs. 9 and 10 further present the histograms of maximum displacement ductility for GM1 and GM2, respectively, when the total number of samples equals 64 and the two ground motions are scaled to achieve nominal ductility of 6. Also presented in Figs. 9 and 10 are the distribution of maximum displacement ductility from MCS for the purpose of comparison. The red lines represent the references of maximum displacement ductility obtained from 100000 times MCS and fitted for generalized lambda distribution. It can be observed in both Figs. 9 and 10 that different nonlinear behavior leads to different statistic distribution for the maximum displacement ductility. It can also be observed that with a total of 64 samples, some cases provide good estimates of distributions from MCS such as case 1 in Fig. 10(a), case 2 in Fig. 9(b), case 3 in Figs. 9(c) and 10(c), and case 6 in Fig. 9(f), while the 64 samples are observed not enough to provide accurate estimates for other cases. These are consistent with the LOO errors observed in Figs. 6 and 7, where PCE meta-models with small LOO errors provide good prediction of maximum displacement ductility. This implies that effective and efficient DoE for SHS of the SDOF structure in Eq. (8c) would enable probabilistic assessment of structural performance through accurate estimation of the mean and the variance for the maximum displacement ductility.

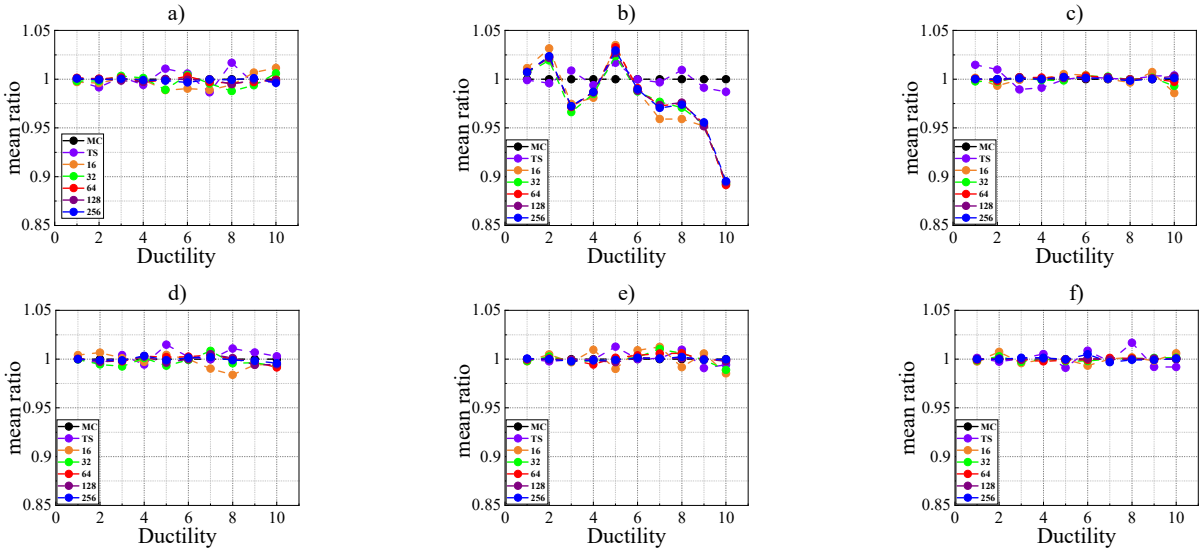

Fig. 11 Comparison of statistic mean for μ with GM1: (a) case 1; (b) case 2; (c) case 3; (d) case 4; (e) case 5; (f) case 6

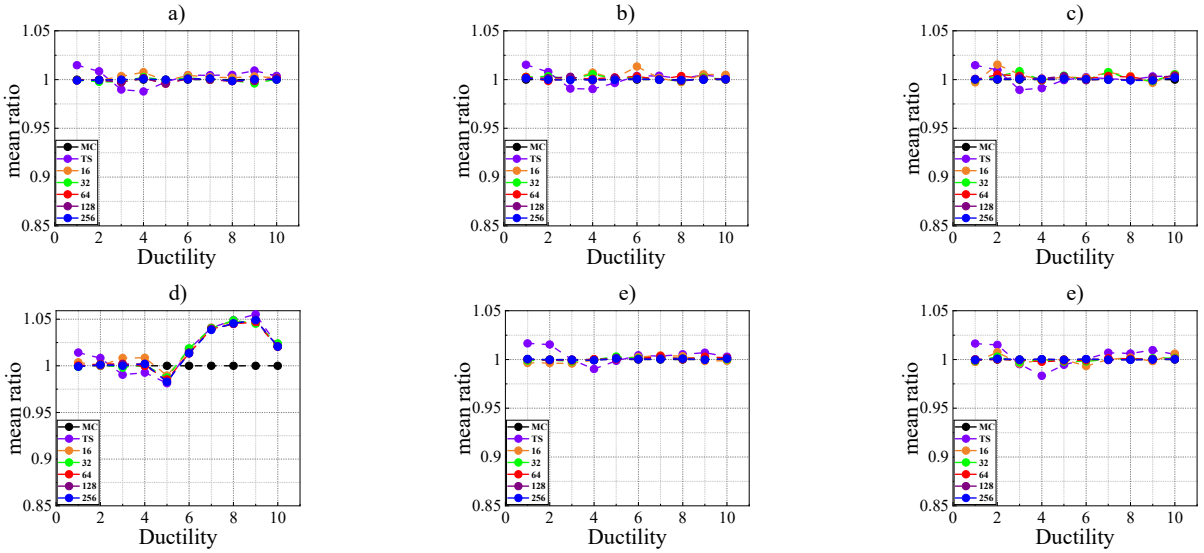

Fig. 12 Comparison of statistic mean for μ with GM2: (a) case 1; (b) case 2; (c) case 3; (d) case 4; (e) case 5; (f) case 6

3.5 Comparison of statistical moments

To further evaluate the efficacy and efficiency of DoE using Sobol sequence, the statistical moments are compared between those from 100000 times MCS, those from PCE meta-modeling, and those calculated directly based on the responses from computational simulation using Sobol sequence samples (referred to as *Training Set*, or *TS*). The ratios of statistical moments (i.e., the mean and variance estimated from the PCE meta-modeling and calculated from the training set) to the corresponding value from MCS are used to evaluate the effect of nonlinear degradation on DoE of SHS using the Sobol Sequence. For different numbers of Sobol Sequence samples, Figs. 11 and 12 present the comparison of statistical means of ductility normalized by the corresponding mean from MCS for the ground motion GM1 and GM2, respectively. It can be observed that for most cases the mean values from PCE meta-modeling have relative errors less than 5% except the case with only strength degradation for GM1 in Fig. 11(b), where the error reaches 11%. This implies that increasing the number of tests generally does not lead to better estimates of mean maximum displacement ductility. A total number of 16 or 32 hybrid simulations will enable researchers to acquire accurate estimate of mean maximum displacement ductility. Even for the outlier case in Fig. 11(b), the maximum relative error reaches 11% when the maximum displacement ductility reaches around 10 and is less than 5% for all other values of μ. This indicates that for the two selected ground motions, the type of nonlinear behavior does not significantly affect the accuracy of estimates for the statistical means using the PCE meta-modeling, and the experimental design of stochastic hybrid simulation for the SDOF structure in Eq. (8a) can ignore the type of nonlinear behavior in the experimental substructure. It can also be observed in Figs. 11 and 12 that estimates of mean maximum displacement ductility directly from training sets has almost same accuracy as those from PCE meta-

Table 7 RMS of relative error for estimated mean of maximum displacement ductility

GM #	Sample #	Case 1	Case 2	Case 3	Case 4	Case 5	Case 6
GM1	TS (64 samples)	0.0274	0.0276	0.0231	0.0216	0.0195	0.0247
	16	0.0241	0.1426	0.0189	0.0225	0.0280	0.0129
	32	0.0199	0.1325	0.0092	0.0171	0.0170	0.0055
	64	0.0075	0.1339	0.0063	0.0113	0.0109	0.0034
	128	0.0063	0.1310	0.0044	0.0111	0.0047	0.0014
	256	0.0056	0.1303	0.0034	0.0066	0.0040	0.0063
GM2	TS (64 samples)	0.0266	0.0232	0.0231	0.0929	0.0269	0.0321
	16	0.0108	0.0173	0.0198	0.0845	0.0092	0.0129
	32	0.0062	0.0080	0.0138	0.0844	0.0048	0.0055
	64	0.0058	0.0065	0.0095	0.0812	0.0051	0.0034
	128	0.0059	0.0043	0.0063	0.0833	0.0027	0.0014
	256	0.0023	0.0017	0.0027	0.0828	0.0019	0.0012

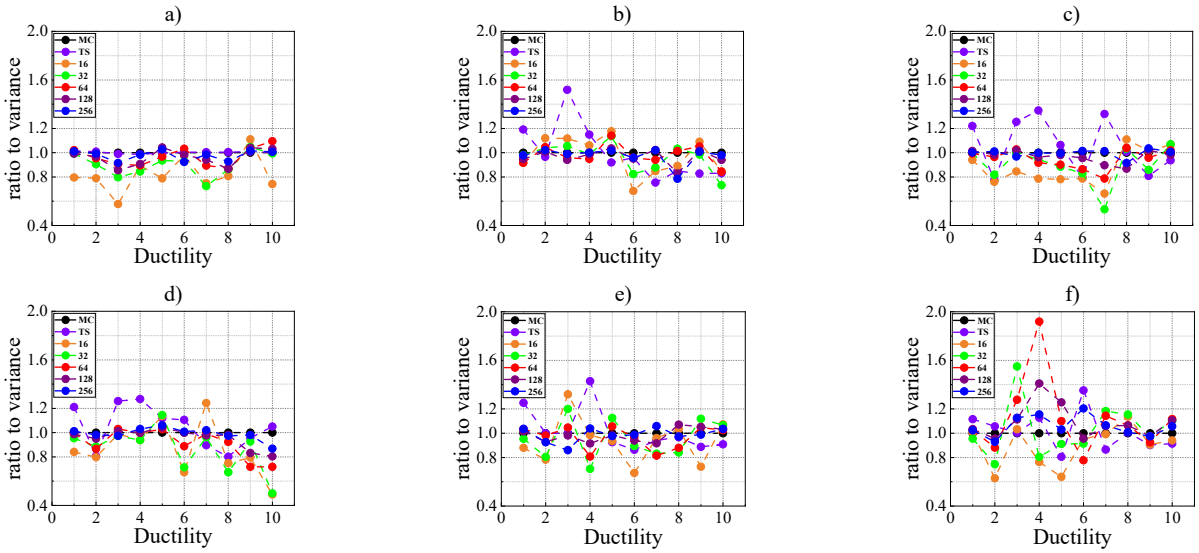

Fig. 13 Comparison of the statistic variance for μ with GM1: (a) case 1; (b) case 2; (c) case 3; (d) case 4; (e) case 5; (f) case 6

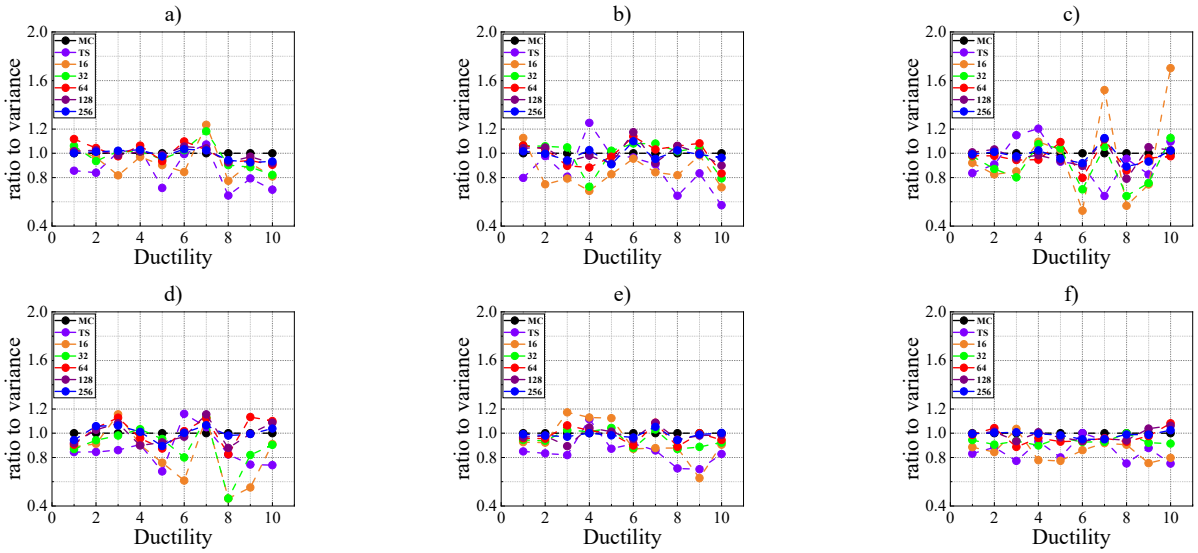

Fig. 14 Comparison of statistic variance for μ with GM2: (a) case 1; (b) case 2; (c) case 3; (d) case 4; (e) case 5; (f) case 6

modeling. Table 7 provides the root mean square (RMS) of the relative error in the estimated mean. Also presented in Table 7 are the relative error of TS using 64 samples

Similarly, using the variance from Monte Carlo simulation as reference, Figs. 13 and 14 present the comparison of statistical variance from PCE meta-model established from different numbers of Sobol Sequence samples for GM1 and GM2, respectively. It can be observed that, unlike the mean displacement ductility demand in Figs. 11 and 12, larger relative errors are observed in the estimation of variance with the maximum value close to 100%. It is worth noting that PCE has a larger relative error in the prediction of variance than mean value. This relative error in variance estimation is observed to vary with respect to the nonlinearity type and the number of Sobol sequence samples. The increase of the number of samples again is observed to not necessarily lead to better accuracy for the estimation. For GM1 as the ground motion input in Fig. 13, the increase of Sobol sequence samples generally reduces the error in the estimation for the variance under different ductility. For case 1 in Fig. 13(a) with minor ductility around 3, the error in variance estimation decreases gradually as 45%, 20%, 10%, 12% and 10% for the number of Sobol samples of 16, 32, 64, 128 and 256, respectively. For case 3 in Fig. 13(c) with moderate ductility around 5, the error in variance estimation decreases gradually as 20%, 10%, 9%, 2% and 1% for the number of Sobol samples of 16, 32, 64, 128 and 256, respectively. For case 5 in Fig. 13(e) with significant ductility around 9, the estimation error in variance decreases as 30%, 15%, 5%, 4% and 1% for the number of Sobol samples of 16, 32, 64, 128 and 256, respectively. When the number of samples is 64, the relative errors in estimation are less than 20% under all different ductility levels, while when the number of samples is 256, the relative errors are all less than 10%.

Therefore, the influence of ductility on the estimation of statistic variance should be considered in the DoE for SHS. Comparing all the six cases in Fig. 13, the estimation errors for case 1 in Fig. 13(a) are observed to have the least variation, while the other five cases in Fig. 13 have much larger variation. For case 2 in Fig. 13(b) and case 6 in Fig. 13(f), the error in variance estimation close to 50% and 100%. This implies that the degradation and pinching have impact on accuracy of the PCE meta-models thus the number of hybrid simulations to acquire accurate estimates of structural response statistics. Also presented in Fig. 13 are the errors of estimation in variance calculated from TS. It can again be observed that estimation from PCE meta-modeling generally provide better accuracy than that from TS.

Similar trends but different values can be observed in Fig. 14 for the error in the estimation for the variance of maximum displacement ductility when GM2 is used as ground motion input. Observation of different errors is consistent with previous observations and can be attributed to the record-to-record variability. Similar trend however implies that findings from this study could provide some general guidance on applying the Sobol sequence to DoE of SHS even different ground motions are used for hybrid simulation. The effect of different nonlinear behavior can be observed from different values of the variance ratio. The ductility is again shown to be influential on the error in variance estimation using Sobol sequence samples. For minor and moderate ductility in Figs. 14(a)~(f), a total of 32 Sobol sequence samples generally enables good estimation in variance with an error less than 20%, and 64 Sobol sequence samples lead to error less than 15%. However, for significant ductility Fig. 14 also shows the estimation in variance over 50% with 16 Sobol sequence samples and a minimum of 128 Sobol sequence samples are necessary for case 3 (stiffness degradation only) and case 4 (both stiffness and strength degradation) to have estimation error less than 20%. Table 8 provides the RMS of the relative error in the variance for maximum displacement ductility in comparison with the relative error for TS using 64 samples. It can again be observed that the RMS error generally decreases with the increase in the number of samples for most cases presented in this study. However, ductility and degradation are observed to have much significant on the number of samples for accurate estimate. The PCE meta-modeling

Table 8 RMS of relative error for estimated variance of maximum displacement ductility

GM #	Sample #	Case 1	Case 2	Case 3	Case 4	Case 5	Case 6
GM1	TS (64 samples)	0.0266	0.6915	0.6894	0.5536	0.5442	0.4801
	16	0.7082	0.4864	0.5952	0.7883	0.6004	0.5974
	32	0.4251	0.3769	0.5672	0.6975	0.5149	0.7006
	64	0.2495	0.2573	0.2938	0.4438	0.3105	1.0193
	128	0.2375	0.2093	0.1828	0.2691	0.1805	0.5189
	256	0.1418	0.2241	0.1001	0.1569	0.1845	0.3102
GM2	TS (64 samples)	0.6241	0.6967	0.5273	0.6081	0.5847	0.5304
	16	0.4686	0.6241	1.1451	0.8830	0.5152	0.5267
	32	0.3140	0.3803	0.5962	0.6417	0.2477	0.2276
	64	0.2299	0.2981	0.3033	0.3431	0.2045	0.1978
	128	0.1390	0.2578	0.2804	0.2782	0.1687	0.1439
	256	0.1308	0.1622	0.2078	0.1669	0.0945	0.0798

provides better accuracy than the Sobol sequence sampling alone.

4. Experimental verification

Hybrid simulations are conducted in laboratories to validate the findings from computation analysis. The prototype structure represents a single-degree freedom shear frame. The frame is assumed to deform in pure shear with rigid beams, as shown in Fig. 15(a). A point of inflection will then develop at mid-height of the story, allowing for the extraction of the single-degree-of-freedom experimental substructure. The mean natural period of the SDOF structure is assumed to be 1 second and the mean viscous damping ratio is 2%. The equation of motion for the hybrid model is solved using Newmark's explicit integration algorithm (Newmark 1959) modified for hybrid simulation through OpenSees (McKenna 2011). The experiments are conducted at the State Key State Key Laboratory of Disaster Reduction in Civil Engineering at Tongji University. The test setup consists of a steel column, an actuator and a steel base beam as shown in Fig. 15(b). Each test specimen consisted of a 1,320 mm long build-up section cantilever column with an idealized plastic hinge connection at the base as shown in Fig. 15(c). And more details of the specimen are shown in Fig. 16. Average initial stiffness of the specimens was approximately 8.082 kN/mm. A testing system based on OpenSees-OpenFresco-MTS controller was constructed for hybrid simulation, where OpenSees is used for numerical calculation, OpenFresco (Schellenberg *et al*. 2007) is used for data interaction as shown in Fig. 17(a), and MTS actuator driven by its controller is used for physical loading as shown in Fig. 17(b). Through MTS interface software CSI, OpenFresco connects OpenSees with MTS controller, which works as data exchange channel from numerical sub-structure to physical sub-structure. The MTS 244.41 servo-hydraulic actuator has a load capacity of 500 kN and displacement stroke of ±250 mm. The actuator is controlled by an MTS FlexTest-100 controller installed in host PC.

Following the discussion in previous sections, the Sobol Sequence are used for the DoE of SHS, i.e., to determine

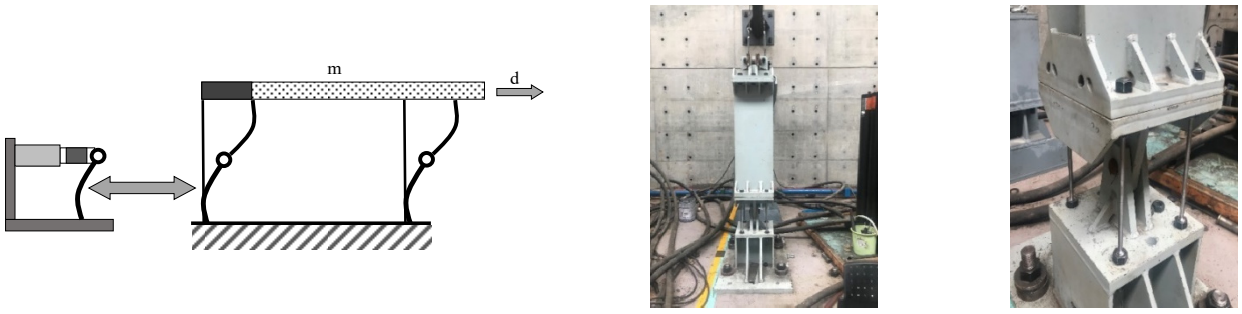

Fig. 15 Laboratory tests: (a) structure model; (b) experimental setup; (c) idealized plastic hinge

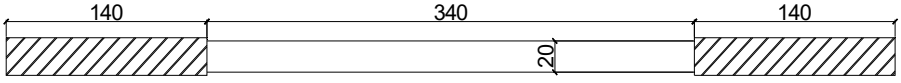

Fig. 16 The basic dimensional data of the specimen (unit: mm)

(a) (b)

Fig. 17 Stochastic hybrid simulation: (a) controller; (b) actuator

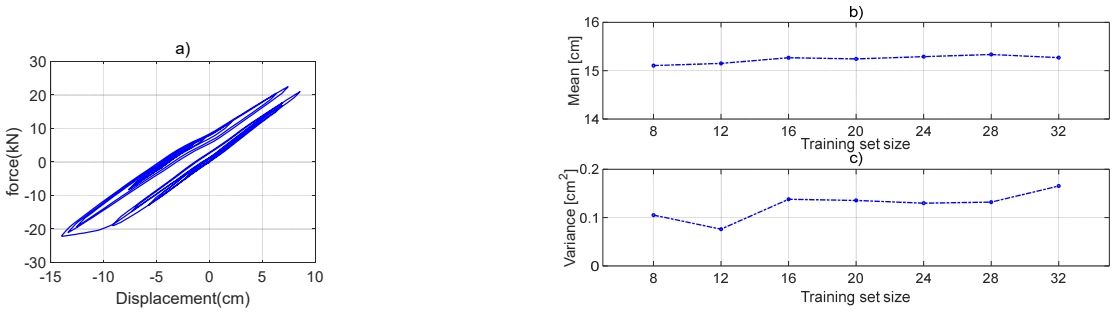

Fig. 18 Results from stochastic hybrid simulation: (a) typical hysteresis behavior; (b) mean; (c) variance

the values of natural frequency and damping ratio of the SDOF structure. Due to the constraints on time and cost, a total of 32 hybrid simulation are carried out for the SDOF structure in the laboratories. The ground motion GM1 used in computational analysis is selected for the experiments. Fig. 18(a) shows the typical hysteresis behavior of the SDOF structure from one hybrid simulation. No significant strength or stiffness degradation or pinching is observed. This might be attributed to the scale of ground motion used in the experiments. It is also worth noting that larger scale of selected ground motion could have also been used which however is found to lead to buckling of threaded bars in the idealized plastic hinge and thus torsion response of the column. The structure is observed to yield around 8 cm and the maximum displacement is around 14 cm. The estimated ductility demand is around 2. Figs. 18(b) and 18(c) present the variation of mean and variance of the maximum displacement with respect to the increase of the number of samples, which are estimated using PCE meta-modeling of the maximum displacements from hybrid simulation. Due to the fact that there is no accurate model for the plastic hinge, there is no reference from MCS for comparison. Though conducting more tests would offer further insight, the current test results are sufficient for the following discussion. It can be observed in Figs. 18(b) and 18(c) that when the number of samples increases to about 30, both estimates of mean and variance steadily converge when the number of samples reaches 32, where the mean and the variances are estimated as 15.3 cm and 0.16 cm^2. The estimates from PCE meta-modeling are again observed to provide better estimate than those directly calculated from measured structural responses. Slight oscillation can also be observed especially in the estimated variance, which however is relatively small when compared with the values of estimated mean and variance. Continuing to increase the number of hybrid tests is therefore not pursued to further reduce these small oscillations.

5. Conclusions

Hybrid simulation provides an efficient and effective experimental technique for performance evaluation of structures especially those close to collapse under earthquakes. This study explores the experimental design of stochastic hybrid simulation to account for uncertainties within substructures through traditional hybrid simulation. A series of hybrid simulation is designed and conducted in laboratory to acquire statistics for structural responses of interest. Computational analysis of a nonlinear single-degree-of-freedom structure is conducted to emulate the hybrid simulation in laboratory. The generalized Bouc-Wen model is adopted to emulate nonlinear close to collapse behavior of strength and stiffness degradation as well as pinching. Two ground motions are used to evaluate the potential influence of record-to-record variation. The meta-modeling approach of polynomial chaos expansion is used to evaluate the efficacy and efficiency of Sobol sequence for DoE of stochastic hybrid simulation. Laboratory experiments are further conducted to validate some findings from the computational analysis.

Based on the observations from both computational analysis and experimental validation, the following conclusions can be drawn: 1) Proper experimental design could enable stochastic hybrid simulation to account for structural uncertainties through a limited number of laboratory tests. This could significantly expand the capacity of traditional hybrid simulation technique. 2)

Sampling structural uncertainties using Sobol sequence provide a decent starting point for experimental design of stochastic hybrid simulation. More specifically, stochastic hybrid simulation using the Sobol sequence provides accurate estimates of mean for structural response of interests. The accuracy is observed to be independent of the input of ground motion, the number of samples, the ductility of structure and the type of structural nonlinearity. 3) The accuracy of variance for structural response however varies for different types of nonlinear behavior, the extent of nonlinear behavior (i.e., ductility) as well as different ground motions. Required number of Sobol samples varies from 32 to 256 to achieve relative error smaller than 10%. 4) Polynomial chao expansion provides a useful meta-modeling tool to estimate the mean and variance of structural response of interest. The leave-one-out error provide a good indicator through cross validation to evaluate the accuracy of the PCE meta-model. 5) The one-stage experimental design using Sobol sequence samples is observed to require various number of hybrid simulation even for a single-degree-of-freedom structure with two sources of uncertainties. Future work will explore adaptive experimental design for stochastic hybrid simulation to account for the Record-to-record variation and structural nonlinearity.

Data availability

Some or all data, models, or code that support the findings of this study are available from the corresponding author upon reasonable request, including all data, models and code.

Acknowledgments

The study has been partially supported by the Ministry of Science and Technology of the People's Republic of China under Grant No. 2018YFE0206100. The opinions and conclusions presented in this paper are those of the authors and do not necessarily reflect the views of the sponsoring organizations.

References

Abbiati, G., Marelli, S., Bursi, O.S., Sudret, B. and Stojadinovic, B. (2015), "Uncertainty propagation and global sensitivity analysis in hybrid simulation using polynomial chaos expansion", *Proceedings of the Fourth International Conference on Soft Computing Technology in Civil*, *Structural and Environmental Engineering*.

Abbiati, G., Marelli, S., Sudret, B. and Stojadinovic, B. (2018), "Hybrid simulation of mechanical systems with uncertain parameters based on surrogate modeling", *Proceedings of the 11th National Conference on Earthquake Engineering*, Los Angeles, CA, USA, June.

Airouche, A., Bechtoula, H., Aknouche, H., Thoen, B.K. and Benouar, D. (2014), "Experimental identification of the six DOF CGS, Algeria, shaking table system", *Smart Struct. Syst.*, *Int. J.*, **13**(1), 137-154. https://doi.org/10.12989/sss.2014.13.1.137

Avci, M., Botelho, R.M. and Christenson, R. (2020), "Real-time hybrid substructuring of a base isolated building considering robust stability and performance analysis", *Smart Struct. Syst.*, *Int. J.*, **25**(2), 155-167. https://doi.org/10.12989/sss.2020.25.2.155

Bernal, D. (1992), "Instability of buildings subjected to earthquakes", *J. Struct. Eng.*, **118**(8), 2239-2260. https://doi.org/10.1061/(ASCE)0733-9445(1992)118:8(2239)

Blatman, G. and Sudret, B. (2010), "An adaptive algorithm to build up sparse polynomial chaos expansions for stochastic finite element analysis", *Probabil. Eng. Mech.*, **25**(2), 183-197. https://doi.org/10.1016/j.probengmech.2009.10.003

Blatman, G. and Sudret, B. (2011), "Adaptive sparse polynomial chaos expansion based on least angle regression", *J. Computat. Phys.*, **230**(6), 2345-2367. https://doi.org/10.1016/j.jcp.2010.12.021

Blanning, R.W. (1975), "The construction and implementation of metamodels", *Simulation*, **24**(6), 177-184. https://doi.org/10.1177/003754977502400606

Bourinet, J.M. (2016), "Rare-event probability estimation with adaptive support vector regression surrogates", *Reliabil. Eng. Syst. Safety*, **150**, 210-221. https://doi.org/10.1016/j.ress.2016.01.023

Casciati, S. and Hamdaoui, K. (2008), "Experimental and numerical studies toward the implementation of shape memory alloy ties in masonry structures", *Smart Struct. Syst.*, *Int. J.*, **4**(2), 153-169. https://doi.org/10.12989/sss.2008.4.2.153

Cha, Y.J., Agrawal, A.K., Friedman, A., Phillips, B., Ahn, R., Dong, B., Dyke, S.J., Spencer, B.F., Ricles, J. and Christenson, R. (2014), "Performance validations of semiactive controllers on large-scale moment-resisting frame equipped with 200-kN MR damper using real-time hybrid simulations", *J. Struct. Eng.*, **140**(10), p. 04014066. https://doi.org/10.1061/(ASCE)ST.1943-541X.0000982

Chae, Y., Ricles, J.M. and Sause, R. (2014), "Large-scale real-time hybrid simulation of a three-story steel frame building with magneto-rheological dampers", *Earthq. Eng. Struct. Dyn.*, **43**(13), 1915-1933. https://doi.org/10.1002/eqe.2429

Chen, P.C. and Chen, P.C. (2020), "Robust stability analysis of real-time hybrid simulation considering system uncertainty and delay compensation", *Smart Struct. Syst.*, *Int. J.*, **25**(6), 719-732. https://doi.org/10.12989/sss.2020.25.6.719

Chen, C., Ricles, J.M., Marullo, T.M. and Mercan, O. (2009), "Real-time hybrid testing using the unconditionally stable explicit CR integration algorithm", *Earthq. Eng. Struct. Dyn.*, **38**(1), 23-44. https://doi.org/10.1002/eqe.838

Chen, C., Ricles, J.M., Karavasilis, T.L., Chae, Y. and Sause, R. (2012), "Evaluation of a real-time hybrid simulation system for performance evaluation of structures with rate dependent devices subjected to seismic loading", *Eng. Struct.*, **35**, 71-82. https://doi.org/10.1016/j.engstruct.2011.10.006

Chen, C., Xu, W., Guo, T. and Chen, K. (2017), "Analysis of actuator delay and its effect on uncertainty quantification for real-time hybrid simulation", *Earthq. Eng. Eng. Vib.*, **16**(4), 713-725. https://doi.org/10.1007/s11803-017-0409-6

Chen, P.C., Hsu, S.C., Zhong, Y.J. and Wang, S.J. (2019), "Real-time hybrid simulation of smart base-isolated raised floor systems for high-tech industry", *Smart Struct. Syst.*, *Int. J.*, **23**(1), 91-106. https://doi.org/10.12989/sss.2019.23.1.091

Chen, M., Guo, T., Chen, C. and Xu, W. (2020), "Data-driven arbitrary polynomial chaos expansion on uncertainty quantification for real-time hybrid simulation under stochastic ground motions", *Experim. Techniq.*, **44**, 751-762. https://doi.org/10.1007/s40799-020-00381-w

Chojaczyk, A.A., Teixeira, A.P., Neves, L.C., Cardoso, J.B. and Soares, C.G. (2015), "Review and application of artificial neural

networks models in reliability analysis of steel structures", *Struct. Safety*, **52**, 78-89. https://doi.org/10.1016/j.strusafe.2014.09.002

Chowdhury, R. and Rao, B.N. (2009), "Assessment of high dimensional model representation techniques for reliability analysis", *Probabil. Eng. Mech.*, **24**(1), 100-115. https://doi.org/10.1016/j.probengmech.2008.02.001

Darby, A.P., Blakeborough, A. and Williams, M.S. (1999), "Real-time substructure tests using hydraulic actuators", *J. Eng. Mech.*, **125**, 1133-1139. https://doi.org/10.1061/(ASCE)0733-9399(1999)125:10(1133)

Dermitzakis, S.N. and Mahin, S.A. (1985), "Development of Substructuring Techniques for On-Line Computer Controlled Seismic Performance Testing", Report UCB/EERC-85/04, Earthquake Engineering Research Center, University of California, Berkeley, CA, USA.

Fang, H. and Horstemeyer, M.F. (2006), "Global response approximation with radial basis functions", *Eng. Optimiz.*, **38**(04), 407-424. https://doi.org/10.1080/03052150500422294

Gao, X., Castaneda, N. and Dyke, S.J. (2013), "Real time hybrid simulation: from dynamic system, motion control to experimental error", *Earthq. Eng. Struct. Dyn.*, **42**(6), 815-832. https://doi.org/10.1002/eqe.2246

Gaspar, B., Teixeira, A.P. and Soares, C.G. (2014), "Assessment of the efficiency of Kriging surrogate models for structural reliability analysis", *Probabil. Eng. Mech.*, **37**, 24-34. https://doi.org/10.1016/j.probengmech.2014.03.011

Goda, K., Hong, H.P. and Lee, C.S. (2009), "Probabilistic characteristics of seismic ductility demand of sdof systems with bouc-wen hysteretic behavior", *J. Earthq. Eng.*, **13**(5), 600-622. https://doi.org/10.1080/13632460802645098

Goel, R.K. and Chopra, A.K. (2004), "Evaluation of modal and FEMA pushover analyses: SAC buildings", *Earthq. Spectra*, **20**(1), 225-254. https://doi.org/10.1193/1.1646390

Guo, T., Xu, W. and Chen, C. (2014), "Analysis of decimation techniques to improve computational efficiency of a frequency-domain evaluation approach for real-time hybrid simulation", *Smart Struct. Syst., Int. J.*, **14**(6), 1197-1220. https://doi.org/10.12989/sss.2014.14.6.1197

Hakuno, M., Shidawara, M. and Hara, T. (1969), "Dynamic destructive test of a cantilever beam, controlled by an analog-computer", *Proceedings of the Japan Society of Civil Eengineers*, Vol. 1969, No. 171, pp. 1-9. https://doi.org/10.2208/jscej1969.1969.171_1

Hashemi, M.J. and Mosqueda, G. (2014), "Innovative substructuring technique for hybrid simulation of multistory buildings through collapse", *Earthq. Eng. Struct. Dyn.*, **43**(14), 2059-2074. https://doi.org/10.1002/eqe.2427

Hayati, S. and Song, W. (2017), "An optimal discrete-time feedforward compensator for real-time hybrid simulation", *Smart Struct. Syst., Int. J.*, **20**(4), 483-498. https://doi.org/10.12989/sss.2017.20.4.483

Hurtado, J.E. and Alvarez, D.A. (2001), "Neural-network-based reliability analysis: a comparative study", *Comput. Methods Appl. Mech. Eng.*, **191**(1-2), 113-132. https://doi.org/10.1016/S0045-7825(01)00248-1

Ibarra, L.F., Medina, R.A. and Krawinkler, H. (2005), "Hysteretic models that incorporate strength and stiffness deterioration", *Earthq. Eng. Struct. Dyn.*, **34**(12), 1489-1511. https://doi.org/10.1002/eqe.495

Iman, R.L., Davenport, J.M. and Zeigler, D.K. (1980), Latin hypercube sampling (program user's guide), OSTI 5571631.

Isukapalli, S.S., Roy, A. and Georgopoulos, P.G. (1998), "Stochastic response surface methods (SRSMs) for uncertainty propagation: application to environmental and biological systems", *Risk Anal.*, **18**(3), 351-363. https://doi.org/10.1111/j.1539-6924.1998.tb01301.x

Jin, R., Chen, W. and Sudjianto, A. (2002), "On sequential sampling for global metamodeling in engineering design", In: *International Design Engineering Technical Conferences and Computers and Information in Engineering Conference*, Vol. 36223, pp. 539-548. https://doi.org/10.1115/DETC2002/DAC-34092

Krawinkler, H. and Seneviratna, G.D.P.K. (1998), "Pros and cons of a pushover analysis of seismic performance evaluation", *Eng. Struct.*, **20**(4-6), 452-464. https://doi.org/10.1016/S0141-0296(97)00092-8

Lee, S.K., Park, E.C., Min, K.W., Lee, S.H., Chung, L. and Park, J.H. (2007), "Real-time hybrid shaking table testing method for the performance evaluation of a tuned liquid damper controlling seismic response of building structures", *J. Sound Vib.*, **302**(3), 596-612. https://doi.org/10.1016/j.jsv.2006.12.006

Lignos, D.G. and Krawinkler, H. (2011), "Deterioration modeling of steel components in support of collapse prediction of steel moment frames under earthquake loading", *J. Struct. Eng.*, **137**(11), 1291-1302. https://doi.org/10.1061/(ASCE)ST.1943-541X.0000376

Lignos, D.G., Moreno, D.M. and Billington, S.L. (2014), "Seismic retrofit of steel moment-resisting frames with high-performance fiber-reinforced concrete infill panels: Large-scale hybrid simulation experiments", *J. Struct. Eng.*, **140**(3), p. 04013072. https://doi.org/10.1061/(ASCE)ST.1943-541X.0000877

Lin, Y.C., Sause, R. and Ricles, J. (2013), "Seismic performance of a large-scale steel self-centering moment-resisting frame: MCE hybrid simulations and quasi-static pushover tests", *J. Struct. Eng.*, **139**(7), 1227-1236. https://doi.org/10.1061/(ASCE)ST.1943-541X.0000661

Mahin, S.A., Shing, P.S.B., Thewalt, C.R. and Hanson, R.D. (1989), "Pseudodynamic test method—current status and future directions", *J. Struct. Eng.*, **115**(8), 2113-2128. https://doi.org/10.1061/(ASCE)0733-9445(1989)115:8(2113)

Marelli, S. and Sudret, B. (2015), "UQLab user manual–Polynomial chaos expansions", In: *Chair of Risk, Safety &Uncertainty Quantification*, ETH Zürich, 0.9-104 edition, pp. 97-110.

Martin, J.D. and Simpson, T.W. (2005), "Use of kriging models to approximate deterministic computer models", *AIAA Journal*, **43**(4), 853-863. https://doi.org/10.2514/1.8650

McKenna, F. (2011), "OpenSees: a framework for earthquake engineering simulation", *Comput. Sci. Eng.*, **13**(4), 58-66. https://doi.org/10.1109/MCSE.2011.66

Mooney, C.Z. (1997), *Monte Carlo Simulation*, Vol. 116, Sage publications.

Mosqueda, G., Stojadinovic, B. and Mahin, S.A. (2007), "Real-time error monitoring for hybrid simulation. Part I: methodology and experimental verification", *J. Struct. Eng.*, **133**(8), 1100-1108. https://doi.org/10.1061/(ASCE)0733-9445(2007)133:8(1100)

Mosqueda, G., Stojadinovic, B. Hanley, J. Sivaselvan, M. and Reinhorn, A.M. (2008), "Hybrid seismic response simulation on a geographically distributed bridge model", *J. Struct. Eng.*, **134**(4), 535-543. https://doi.org/10.1061/(ASCE)0733-9445(2008)134:4(535)

Nakashima, M. (2001), "Development, potential, and limitations of real–time online (pseudo–dynamic) testing", *Philosophical Transactions of the Royal Society of London. Series A: Mathematical, Physical and Engineering Sciences*, **359**(1786), 1851-1867. https://doi.org/10.1098/rsta.2001.0876

Nakashima, M. (2020), "Hybrid simulation: An early history", *Earthq. Eng. Struct. Dyn.*, **49**(10), 949-962. https://doi.org/10.1002/eqe.3274

Nakashima, M., Kato, H. and Takaoka, E. (1992), "Development of real-time pseudo dynamic testing", *Earthq. Eng. Struct. Dyn.*, **21**(1), 79-92. https://doi.org/10.1002/eqe.4290210106

Nakashima, M., Matsumiya, T., Suita, K. and Liu, D. (2006), "Test on full-scale three-storey steel moment frame and assessment of ability of numerical simulation to trace cyclic inelastic behaviour", *Earthq. Eng. Struct. Dyn.*, **35**(1), 3-19. https://doi.org/10.1002/eqe.528

Nakata, N. and Stehman, M. (2014), "Compensation techniques for experimental errors in real-time hybrid simulation using shake tables", *Smart Struct. Syst., Int. J.*, **14**(6), 1055-1079. https://doi.org/10.12989/sss.2014.14.6.1055

Nakata, N., Spencer Jr, B.F. and Elnashai, A.S. (2007), "Multi-dimensional mixed-mode hybrid simulation control and applications", *Newmark Structural Engineering Laboratory*. University of Illinois at Urbana-Champaign.

Nakata, N., Dyke, S., Zhang, J., Mosqueda, G., Shao, X., Mahmoud, H., Head, M.H., Bletzinger, M., Marshall, G.A., Ou, G. and Song, C. (2014), Hybrid Simulation Primer and Dictionary. https://datacenterhub.org/resources/8102

Newmark, N.M. (1959), "A method of computation for structural dynamics", *J. Eng. Mech. Div.*, **85**(3), 67-94. https://doi.org/10.1061/JMCEA3.0000098

Niederreiter, H. (1992), *Random number generation and quasi-Monte Carlo methods*, Society for Industrial and Applied Mathematics.

Ramos, M.D.C., Mosqueda, G. and Hashemi, M.J. (2016), "Large-scale hybrid simulation of a steel moment frame building structure through collapse", *J. Struct. Eng.*, **142**(1), 04015086. https://doi.org/10.1061/(ASCE)ST.1943-541X.0001328

Schellenberg, A., Mahin, S.A. and Fenves, G.L. (2007), "A software framework for hybrid simulation of large structural systems", In: *Structural Engineering Research Frontiers*, pp. 1-16. https://doi.org/10.1061/40944(249)3

Shao, X., Reinhorn, A.M. and Sivaselvan, M.V. (2011), "Real-time hybrid simulation using shake tables and dynamic actuators", *J. Struct. Eng.*, **137**(7), 748-760. https://doi.org/10.1061/(ASCE)ST.1943-541X.0000314

Shao, X., van de Lindt, J., Bahmani, P., Pang, W., Ziaei, E., Symans, M., Tian, J. and Dao, T. (2014), "Real-time hybrid simulation of a multi-story wood shear wall with first-story experimental substructure incorporating a rate-dependent seismic energy dissipation device", *Smart Struct. Syst., Int. J.*, **14**(6), 1031-1054. https://doi.org/10.12989/sss.2014.14.6.1031

Shen, S.D., Pan, P., Li, W.F., Miao, Q.S. and Gong, R.H. (2019), "Test on the anchoring components of steel shear keys in precast shear walls", *Smart Struct. Syst., Int. J.*, **24**(6), 783-791. http://doi.org/10.12989/sss.2019.24.6.783

Silva, C.E., Gomez, D., Maghareh, A., Dyke, S.J. and Spencer Jr, B.F. (2020), "Benchmark control problem for real-time hybrid simulation", *Mech. Syst. Signal Process.*, **135**, 106381. https://doi.org/10.1016/j.ymssp.2019.106381

Sivaselvan, M.V. and Reinhorn, A.M. (2000), "Hysteretic models for deteriorating inelastic structures", *J. Eng. Mech.*, **126**(6), 633-640. https://doi.org/10.1061/(ASCE)0733-9399(2000)126:6(633)

Sobol, I.M. (1993), "Sensitivity estimates for nonlinear mathematical models", *Math. Model. Comput. Exp.*, **1**(4), 407414.

Song, J.K. and Pincheira, J.A. (2000), "Spectral displacement demands of stiffness-and strength-degrading systems", *Earthq. Spectra*, **16**(4), 817-851. https://doi.org/10.1193/1.1586141

Stojadinovic, B., Mosqueda, G. and Mahin, S.A. (2006), "Event-driven control system for geographically distributed hybrid simulation", *J. Struct. Eng.*, **132**(1), 68-77. https://doi.org/10.1061/(ASCE)0733-9445(2006)132:1(68)

Takizawa, H. and Jennings, P.C. (1980), "Collapse of a model for ductile reinforced concrete frames under extreme earthquake motions", *Earthq. Eng. Struct. Dyn.*, **8**(2), 117-144. https://doi.org/10.1002/eqe.4290080204

Vamvatsikos, D. and Cornell, C.A. (2002), "Incremental dynamic analysis", *Earthq. Eng. Struct. Dyn.*, **31**(3), 491-514. https://doi.org/10.1002/eqe.141

Villaverde, R. (2007), "Methods to assess the seismic collapse capacity of building structures: State of the art", *J. Struct. Eng.*, **133**(1), 57-66. https://doi.org/10.1061/(ASCE)0733-9445(2007)133:1(57)

Vian, D. and Bruneau, M. (2003), "Tests to structural collapse of single degree of freedom frames subjected to earthquake excitations", *J. Struct. Eng.*, **129**(12), 1676-1685. https://doi.org/10.1061/(ASCE)0733-9445(2003)129:12(1676)

Wang. T., Nakashima, M. and Pan, P. (2006), "On-line hybrid test combining with general-purpose finite element software", *Earthq. Eng. Struct. Dyn.*, **35**(12), 1471-1488. https://doi.org/10.1002/eqe.586

Wang, T., McCormick, J., Yoshitake, N., Pan, P., Murata, Y. and Nakashima, M. (2008), "Collapse simulation of a four-story steel moment frame by a distributed online hybrid test", *Earthq. Eng. Struct. Dyn.*, **37**(6), 955-974. https://doi.org/10.1002/eqe.798

Wang, Z., Wu, B., Bursi, O.S., Xu, G. and Ding, Y. (2014), "An effective online delay estimation method based on a simplified physical system model for real-time hybrid simulation", *Smart Struct. Syst., Int. J.*, **14**(6), 1247-1267. https://doi.org/10.12989/sss.2014.14.6.1247

Wang, Z., Xu, G., Li, Q. and Wu, B. (2020a), "An adaptive delay compensation method based on a discrete system model for real-time hybrid simulation", *Smart Struct. Syst., Int. J.*, **25**(5), 569-580. https://doi.org/10.12989/sss.2020.25.5.569

Wang, Z., Tan, Q., Shi, P., Yang, G., Zhu, S., Xu, G., Wu, B. and Sun, J. (2020b), "Performance validation and application of a mixed force-displacement loading strategy for bi-directional hybrid simulation", *Smart Struct. Syst., Int. J.*, **26**(3), 373-390. https://doi.org/10.12989/sss.2020.26.3.373

Wiener, N. (1938), "The homogeneous chaos", *Am. J. Mathe.*, **60**(4), 897-936. https://doi.org/10.2307/2371268

Wu, B. and Wang, T. (2014), "Model updating with constrained unscented Kalman filter for hybrid testing", *Smart Struct. Syst., Int. J.*, **14**(6), 1105-1129. https://doi.org/10.12989/sss.2014.14.6.1105

Wu, B., Xu, G., Wang, Q. and Williams, M.S. (2006), "Operator-splitting method for real-time substructure test", *Earthq. Eng. Struct. Dyn.*, **35**(3), 293-314. https://doi.org/10.1002/eqe.519

Xiu, D. and Karniadakis, G.E. (2002), "The Wiener--Askey polynomial chaos for stochastic differential equations", *SIAM J. Scientif. Comput.*, **24**(2), 619-644. https://doi.org/10.1137/S1064827501387826

BS